Transient thermal behaviour of crumb rubber-modified concrete and implications for thermal response and energy efficiency in buildings

Matthew R Hall [a] *, Khalid B Najim [a], and Christina J Hopfe [b]

[a] Nottingham Centre for Geomechanics, Division of Materials, Mechanics and Structures, Faculty of Engineering, University of Nottingham, University Park, Nottingham NG7 2RD, UK, Tel: +44 (0) 115 846 7873, Fax: +44 (0) 115 951 3159, E-mail: matthew.hall@nottingham.ac.uk

[b] BRE Institute of Sustainable Engineering, School of Engineering, Cardiff University, The Parade, Cardiff, CF24 3AA, UK,

*corresponding author

Abstract

Experimental data is presented for the dry and saturated steady state thermo-physical properties, and also the dynamic thermal properties, of 180, 120 and 65 mm target slump mix designs for Plain Rubberised Concrete (PRC) with varying %wt rubber substitution and aggregate replacement types (fine, coarse, and mixed). The composites had significantly lower density and thermal conductivity than plain concrete, and there was an inverse relationship between thermal admittance and (a) mix design target slump, and (b) %wt crumb rubber substitution. The thermal decrement remained almost constant, and yet the associated time lag can be increased significantly. Parametric analysis of the effects of crumb rubber substitution for a heavyweight PassivHaus standard dwelling (in non-mechanical ventilation mode) was conducted using building performance simulation. For a London (warmer) or Glasgow (cooler) climate, PRC can be used at up to 30%wt addition and all replacement types as a substitute for plain concrete without causing any significant difference in Dry Resultant Temperature (DRT) fluctuation, if used in conjunction with passive ventilation for night time cooling. However, for the same material there was a general tendency to increase the number of overheating hours in this construction type due to its greater ability to retain any stored heat energy

Keywords: thermo-physical properties; rubberised concrete; transient numerical modelling; building performance simulation; energy efficiency

Nomenclature

c_{dry}	dry state specific heat capacity	J/(kg·K)
c_{sat}	saturated state specific heat capacity	J/(kg·K)
f	decrement factor	-
F	surface factor	-
	mean temperature	ºC
HFM	heat flow meter output	mV
q_{is}	internal surface heat flux	W/m^2
q_{es}	external surface heat flux	W/m^2
n_{ap}	apparent porosity	%
T_{ei}	internal environmental temperature	°C
T_{eo}	external environmental temperature	°C
U	Thermal transmittance	$W/(m^2·K)$
Y	Thermal admittance	$W/(m^2·K)$
κ	surface heat capacity (100mm depth)	$kJ/(m^2·K)$
κ_{30}	surface heat capacity (30mm depth)	$kJ/(m^2·K)$
λ_{dry}	dry state thermal conductivity	W/(m·K)
λ_{sat}	saturated state thermal conductivity	W/(m·K)
ρ_{dry}	dry density	kg/m^3
ρ_{sat}	saturated density	kg/m^3
ϕ	thermal admittance time lag	hr
ψ	surface factor time lag	hr
ω	decrement factor time lag	hr

1. Introduction

To rationalise mean annual operational energy consumption in residential buildings, the relative importance of both heating and cooling loads changes according to the climate for which the building has been designed to operate within its lifetime [1] and [2]. The design of optimum building fabric performance therefore requires a trade-off between dynamic thermal behaviour (temperature buffering and thermal storage) and thermal resistance to heat transfer, where for example a combination of minimal thermal storage but high thermal resistance is required in a climate where the heating load dominates such as the UK [3] and [4]. Here, the vast majority of existing and future planned residential buildings (up to 2050) are in the south east of England (including outer London) where some degree of thermal storage and buffering is required for optimised fabric design and minimised annual energy use for combined heating/cooling loads [5]. However, without significant diurnal temperature variation and the ability to purge the stored heat (e.g. by night time ventilation cooling strategies), thermally massive structures may offer limited benefit particularly in Urban Heat Island (UHI) contexts such as central London where the delayed onset of cooling due to high mass and the heat island lag may actually lead to increased thermal discomfort at the time occupants are most sensitive to it.

Concrete, (in block, monolithic and Insulate Concrete Formwork (ICF) configurations) is one of the mostly widely used materials for load bearing external walls and/or internal partitions where high 'thermal mass' is required for incorporation into the wall fabric design. Plain Rubberised Concrete (PRC) is an ordinary strength (low-high slump) class of concrete with coarse and/or fine rubber aggregate (chipped, crumb or fibre) replacement. A detailed review of research relating to these materials was recently produced by Najim and Hall [6]. PRC typically has good properties in terms of thermal and acoustic resistance, kinetic/vibrational energy absorption, impact resistance, and dynamic mechanical properties [2], [7], [8], [9], [10], [11], [12],[13], [14] and [15]. An added advantage to PRC is that the vast accumulation of end-of-life vehicle tyres presents serious environmental problems [16] leading to an EU ban on stockpiling since 2006 [17] and efforts being made to utilise them in beneficial manner, e.g. as alternative aggregates that (in the UK) avoids landfill and primary aggregates levy taxation. The potential for leachate formation or off-gassing from crumb rubber aggregates, when incorporated in concrete, has not been the subject of a previous research study and could be considered.

The vast majority of research studies have evaluated the mechanical and fresh properties of PRC materials[6], and only a limited number of handful studies have examined their thermal properties [2], [18] and [19]. Concrete thermal conductivity is mainly dependent on the pore moisture content and aggregate volume fraction, and (to a lesser degree) also on age, water/cement ratio, and admixture type(s) [20] and [21] in addition to the measuring equipment itself [22]. Not only does the aggregate %wt content affect the thermo-physical properties of concrete but also the type of aggregate (i.e. density, thermal conductivity, heat capacity) [23].

The aim of this study was to experimentally characterise the thermo-physical properties of PRC concrete materials by investigating the influence of basic mix design (target slump), %wt crumb rubber replacement, and aggregate replacement type, i.e. coarse replacement (CR), fine replacement (FR), and 50:50 fine and coarse replacement (CFR). These basic properties could then be used to determine and evaluate the dynamic thermal characteristics of PRC wall elements in terms of thermal storage and temperature buffering. Finally, the relative performance of each PRC material on the operational energy efficiency in buildings would be determined by using dynamic building performance simulation to accurately assess the usage of rubberised concrete classes in the context of a thermally heavyweight PassivHaus construction type in a number of different scenarios. A previously validated test case building was used, further details of which are given in Section 5.

2. Materials specification and mix design

A previous study by the authors [24] has shown that structural concrete (f'_c > 17 MPa, ρ_d = ≥2000 kg/m^3) can be designed with aggregate substitution by crumb rubber up to 20%wt FR, or up ~15%wt CR and CFR replacement types. Potentially, up to 30%wt of all replacement types could be used for non-structural applications e.g. lightweight block partitions. This research has also shown that the addition of crumb rubber aggregate has a significant effect on concrete mix air entrapment, and as a result provides a reduced slump whilst maintaining a high compaction factor in the plastic state. However, the effects of this on dynamic thermal properties and behaviour have not been studied previously.
For the materials used in this study, high strength (52.5 MPa) CEM I class Portland cement was used, with 10 mm quartzite natural gravel (G = 2.60, A = 1.2), and 5 mm down natural grit sand (G = 2.65, A = 1.1%), both sourced from Hope Valley, UK. In addition, 2–6 mm regular crumb rubber particles sourced from J Allcock & Sons, Manchester, UK. Three types of PRC mix designs were tested based on three different target slump values; high (180 mm), medium (120 mm), and low (65 mm). For each slump level the %wt crumb rubber aggregate replacement was varied between 10%wt, 20%wt, and 30%wt for FR, CR, and CFR, plus a control mix with 0% replacement, giving a total of thirty mixes. For this study, specimens were prepared as 300 × 300 mm slabs with a thickness of 50 mm, based on ASTM C 192-88 [25], and covered by a polyethylene sheet until final setting had occurred (24 h ±2), after which the samples were de-moulded, labelled and submersed in a temperature-controlled water curing tank at 20 °C ± 2 for 28 days. The particle-size distribution and specific surface area for the fine aggregate (FA), coarse aggregate (CA), and crumb rubber aggregate are presented in a previous study [24] along with experimental data for compaction factor, compressive strength (f'_c), and indirect tensile (splitting) strength, dynamic Modulus of Elasticity (E_d), and Ultrasonic Pulse Velocity (UPV). In addition to this, the chemical composition and physical properties of the crumb rubber are also provided elsewhere [24].

3. Characterisation of thermo-physical properties

The specific heat capacity, c_p of each mix design was calculated as the sum of constituent heat capacities and weighted by their %wt proportions. The experimental values for the natural aggregate, crumb rubber, and Hardened Cement Paste (HCP) were presented in a previous study [26], where the mean value of five readings was taken across the range −13 °C to 57 °C and determined using a Differential Scanning Calorimeter (Q10 DSC, TA Instruments). In the dry state, air within open voids was assumed to have negligible heat capacity since it has a density of ~1.205 kg/m^3 at ambient temperatures and is assumed to have zero mass for the purposes of gravimetric material bulk density calculations. The specific heat capacity of concrete in both the dry (c_p) and moisture-dependent state (c_p^*) are calculated from Eqs.(2) and (3), respectively [27].

Eq. 1

Eq. 2

The dry and saturated state specific heat capacities for each of the thirty (reference and PRC) mixes used for this study are given in Table 1, Table 2 and Table 3, corresponding to slump values of 180, 120 and 65, respectively. The thermal conductivity of concrete specimens, following immersion in water (λ^*) and oven-dried (λ) conditions, were experimentally determined using a computer-controlled P.A. Hilton B480 uni-axial heat flow meter apparatus with downward vertical heat flow, which complies with ISO 8301: 2010 [28]. Two slabs with dimensions of 300 × 300 mm, and a typical thickness of 50 mm, were prepared for each mix design and the mean average of two readings were obtained per slab specimen in both oven-dried and saturated states. For thermal conductivity measurement in saturated state, the concrete slabs were removed from the curing tank at the end of their 28-day curing period and sealed in a vapour-tight envelop to prevent any change in moisture content. The influence of the thin envelop on the thermal conductivity of the slab specimens was found to be negligible when measuring thermal conductivity at a steady state variance of 2–3%, as prescribed by ISO 8301: 2010 [28]. In the dry state, all specimens were oven dried at 105 ± 5 °C until the variation in mass was less than 0.2% over a 24 h period, before cooling to ambient laboratory temperature in a desiccator prior to testing. The thermal conductivity is calculated from the apparatus output using the following equation [29]:

$$\lambda = \frac{(d * \left[\left(k1 + (k2 * \bar{T}) + \left((k3 + (k4 * \bar{T})\right) * HFM\right) + \left((K5 + (k6 * \bar{T})) * HFM\right)\right]\right)}{dT}$$

Calibration constants ($k1 - k6$) are determined prior to testing using standard reference specimens of know thermal conductivity determined by an absolute method. The thermo-physical characteristics of PRC materials are quite unusual since the effect of crumb rubber replacement appears to be a reduction in thermal conductivity but an increase in heat capacity. The reduction in conductivity can be attributed partly to the air entrapment effect of non-wetting rubber particles, resulting in significantly increased apparent porosity, but also to the lower thermal conductivity of crumb rubber particles themselves. In higher rubber replacement mixes the relative increase in saturated state thermal conductivity compared with dry state is due to the increased apparent porosity giving greater natural convection heat flow within the pore network when filled with water. Despite the associated reductions in bulk density with rubber replacement, the higher specific heat capacity of rubber particles gives an overall increase in heat capacity for the PRC materials (seeTable 1, Table 2 and Table 3). The implications of these results are that PRC materials could be useful for building fabric to reduce thermal transmittance whilst enhancing thermal buffering.

4. Dynamic thermal admittance properties

These were determined for a 100 mm thick solid concrete exposed external wall, based on ISO 13790: 2004[30], and the 'Dynamic Thermal Properties Calculator' software tool [31]. The calculations assumed a vertical wall with horizontal heat flow and conventional surface boundary layer heat transfer coefficients ofR_{si} = 0.13 m^2 K/W, and R_{so} = 0.04 m^2 K/W, taken from ISO 6946: 2007 [32]. The values for all %wt crumb rubber replacement amounts and aggregate types, for 180 mm, 120 mm and 65 mm slump PRC mix designs, are given in Table 4, Table 5 and Table 6, respectively. The *Y*-value of all three reference mixes is very similar, and the effect of crumb rubber replacement appears to reduce *Y* whilst increasing associated lead time. This suggests that the use of PRC materials for exposed internal fabric may have a slightly lower heat flux from the internal environmental node and at a slower rate. Therefore, in climates where the cooling season dominates annual mean operational energy use, the reduction in the annual load as a result of passive cooling could be slightly lower assuming surface area and wall thickness are constant.

Another interesting effect of rubber replacement is that thermal decrement remains almost constant in all cases, whilst the associated time lag increases but the *U*-value decreases. This suggests that for heat exchange between the internal environmental node and the sol-air node (in either direction), higher rubber content in PRC walls reduces the total heat flux and the rate of change in heat flux as a result of internal/external temperature fluctuation, i.e. a higher thermal buffering effect. This dynamic thermal response is illustrated by the graphs shown in Fig. 1, Fig. 2 and Fig. 3, representing each of the three mix classes. There appears to be no significant difference in internal environmental node temperature fluctuation. However, an increase in %wt rubber replacement appears to cause a significant and proportional reduction in internal surface heat flow, peaking at almost a 1 W/m^2 K reduction at 30%CR or CFR replacement in all three slump classes. This behaviour appears to be due to the fact that rubber aggregate substitution produces PRC materials with increased thermal resistance but also increases volumetric heat capacity, in comparison with plain concrete materials..

5. Transient numerical modelling of thermal behaviour

It was hypothesised that whilst PRC walls offer improved decrement time lag for thermal mass applications, if they are used in highly insulated buildings with low air infiltration, and reduced ventilation rates, then the reduced thermal admittance could increase their susceptibility to overheating. Therefore, the purpose of the numerical modelling was to accurately assess the usage of rubberised concrete classes in the context of a thermally heavyweight PassivHaus construction type in a number of different scenarios. The opaque elemental *U*-values for a PassivHaus must be ≤0.15 W/m^2 K, whilst glazed elements must have a combined (frame and glazing) *U*-value of ≤0.8 W/m^2 K [33]. The dwelling modelled in this study was a two bedroom, two storey (70 m^2) terraced house with two occupants and the potential to be volume-built whilst being compatible with current UK housing typologies and trends [34]. The design layout, main dimensions, and fabric *U*-values for the building are shown in Fig. 4. The cross-sectional wall design and assumed boundary layer values are given in Fig. 5. Comparative analysis was achieved by substituting the 100 mm concrete block used in both the inner and outer leaf for PRC materials. An internal heat gain assumption of 2.1 W/m^{2}was used, and also a standardised room temperature heating set point of 20 °C maintained throughout the heating season.

In the UK, CIBSE Test Reference Year (TRY) weather datasets are typically used to represent an average weather year in dynamic thermal simulations and are based on a composite of twelve average months of data selected from the past twenty years of synoptic readings [35]. However, with global air temperature following a predominantly rising trend for over half a century the use of a TRY which is based on a twenty year historic average implies that the ‘current’ TRY dataset is actually ten years out of date [34]. The use of Design Summer Year (DSY) as opposed to TRY data to some extent buffers the current overheating predictions in the sense that the DSY data theoretically models a hotter than ‘average’ summer, by selecting the median upper quartile summer from the past twenty years of data. In a twenty year dataset this equates to the third hottest summer. The DSY dataset is however likely to provide climatic data which is reasonably representative of the present day situation and for this reason it has been selected as the most accurate data available for the base reference year here, in lieu of the TRY. The Dry Resultant Temperature (DRT) or ‘operative temperature’ is composed of the average of the internal air temperature and the mean room radiant surface temperature [36]. As such the DRT creates a single index temperature which is thought to provide a better indication of thermal comfort than indoor air temperature alone, since radiative surface temperatures are also known to influence the perception of thermal comfort [36]. As a result the DRT system has been adopted as a key thermal index by CIBSE for moderate thermal environments and is also used in various ISO, ANSI/ASHRAE standards [37].

IES-ve Apache was chosen for the dynamic thermal modelling software as it enabled a detailed interrogation of the thermal comfort levels in each PassivHaus construction type to be determined on the basis of its thermal response. Two modelling scenarios were designed to evaluate the potential overheating risk for the dwelling:

Scenario 1: this examined the implications of a present day hotter than average summer on overheating risk using the current CIBSE DSY, using natural ventilation with windows opening when external temperatures reach 23 °C being fully open at 27 °C and closing again at 22 °C was specified in order to replicate a natural tendency to open windows in warm weather.

Scenario 2: this examined the implications of a present day hotter than average summer on overheating risk using the current CIBSE DSY, without night ventilation. In both scenarios, twelve concrete materials were tested including the reference mix, 30%FR, 30%CR, and 30%CFR variants of the 65, 120 and 180 mm slump mix designs.

The use of PRC wall fabric appears to maintain a slightly higher internal DRT, even in a cooler climate (seeFig. 6). This most likely occurs since volumetric heat capacity increases with %wt rubber addition whilst thermal admittance decreases, hence the wall stores slightly more heat energy and offers greater resistance to heat exchange with the indoor environment. However, for this building type the changes in DRT, as a result of selecting PRC over plain concrete for the wall fabric, appears to be insignificant. Fig. 7 shows that as the slump of concrete mix design is decreased, the number of annual overheating hours significantly decreases in Scenario 1 but not in Scenario 2. This finding aligns well with the measured thermal conductivity and admittance values, suggesting that when combined with night time ventilation these materials are able to release a larger quantity of stored heat and so have greater cooling capacity for the following day. As expected, this behaviour is not observed in Scenario 2. The addition of crumb rubber appears to increase the number of overheating hours, particularly in Scenario 1, where the highest number is for 30%CFR 180 mm slump, and the lowest is for the 65 mm slump reference mix. This correlates well with the previous observation (above) and also the inverse relationship between thermal admittance and (a) the mix design target slump, and (b) the %wt crumb rubber substitution.

Scenarios 1 and 2 were repeated for present day base case evaluation of overheating risk based on two cooler climatic scenarios using (a) the current CIBSE TRY weather data for London, and (b) Glasgow. In both cases material selection was restricted to 30%CFR 180 mm slump (highest overheating hours) and 65 mm slump reference mix (lowest overheating hours). As Fig. 6 shows, London TRY was significantly lower than for DSY. For Scenario 1, the number of overheating hours equalled zero in both cases with the exception of the 30%CFR 180 mm slump case for Glasgow which had just 13 h overheating (above 26 °C).

6. Conclusions

The substitution of crumb rubber for mineral aggregate in concrete appears to cause a significant reduction in thermal conductivity, which can be partly attributed to increased air entrapment caused by the non-wetting rubber particles during mixing, and partly to the lower thermal conductivity of the crumb rubber particles. As the %wt addition of crumb rubber increases, there is a greater moisture-dependent effect on the saturated state thermal conductivity due to the increased apparent porosity caused by air entrapment. There appears to be an inverse relationship between the thermal admittance of concrete and both (a) the mix design target slump value, and (b) the %wt crumb rubber substitution. Whilst the volumetric heat capacity of concrete increases with %wt rubber addition, thermal admittance decreases and hence a PRC wall can store more heat energy but offers greater resistance to exchange of that heat with the surrounding environment. A further interesting effect of the rubber is that thermal decrement remains almost constant regardless of the %wt rubber addition, and yet the associated time lag increases significantly.

For a London (warmer) or Glasgow (cooler) climate, PRC can be used (at up to 30%wt addition and all replacement types) as a substitute for plain concrete in heavyweight wall fabric for PassivHaus standard construction without causing any significant difference in DRT fluctuation, if used in conjunction with passive ventilation for night time cooling. This is achieved despite the significantly lower density of PRC concrete. However, PRC has a general tendency to increase the number of overheating hours in this construction type due to its greater ability to retain any stored heat energy. Further research of other building typologies is required to better understand how the unique thermo-physical behaviour of PRC materials can be better exploited.

Acknowledgements

The authors wish to acknowledge the support of the Iraqi Government for the research scholarship enabling this work to be conducted as part of a larger research project.

References

1. Al-Hadhrami, L. M., and A. Ahmad, Assessment of thermal performance of different types of masonry bricks used in Saudi Arabia. Applied Thermal Engineering, 2009. 29(5-6): p. 1123-1130.

2. Dong, Z., et al., Development of thermal energy storage concrete Cement and Concrete Research, 2004. 34: p. 927-934.

3. Al-Jabri, K.S., et al., Concrete blocks for thermal insulation in hot climate. Cement and Concrete Research, 2005. 35(8): p. 1472-1479.

4. Sukontasukkul, P., Use of crumb rubber to improve thermal and sound properties of pre-cast concrete panel. Construction and Building Materials, 2009. 23(2): p. 1084-1092.

5. Rashad, A.M. and S.R. Zeedan, The effect of activator concentration on the residual strength of alkali-activated fly ash pastes subjected to thermal load. Construction and Building Materials. In Press, Corrected Proof.

6. Turgut, P. and B. Yesilata, Physico-mechanical and thermal performances of newly developed rubber-added bricks. Energy and Buildings, 2008. 40(5): p. 679-688.

7. Najim, K.B. and M.R. Hall, A review of the fresh/hardened properties and applications for plain (PRC) and self-compacting rubberised concrete (SCRC). Construction and Building Materials, 2010. 24(11): p. 2043-2051.

8. Ganjian, E., M. Khorami, and A.A. Maghsoudi, Scrap-tyre-rubber replacement for aggregate and filler in concrete. Construction and Building Materials, 2009. 23(5): p. 1828-1836.

9. Paine, K. and R.K. Daher, Research on new applications for granulated rubber in concrete Proceedings Institution of Civil Engineers 2010. 163(CM1): p. 7-17.

10. Yesilata, B. and P. Turgut, A simple dynamic measurement technique for comparing thermal insulation performances of anisotropic building materials. Energy and Buildings, 2007. 39(9): p. 1027-1034.

11. dos Santos, W.N., Effect of moisture and porosity on the thermal properties of a conventional refractory concrete. Journal of the European Ceramic Society, 2003. 23(5): p. 745-755.

12. Kim, K.-H., et al., An experimental study on thermal conductivity of concrete. Cement and Concrete Research, 2003. 33(3): p. 363-371.

13. Neville, A.M., Properties of Concrete, ed. t. Ed. 1995, London: Longman.

14. Khan, M.I., Factors affecting the thermal properties of concrete and applicability of its prediction models. Building and Environment, 2002. 37(6): p. 607-614.

15. BS 882, B., Specification for aggregates from natural sources for concrete 1992.

16. BSEN450-1:2005, Fly ash for concrete —Part 1: Definition, specifications and conformity criteria. British Standard 2005.

17. EFNARC, The European Guidelines for self-compacting concrete: specification, production, and use. 2005: p. 68.

18. Feist et al. Passive House Planning Package. English edition. PassivHaus Institut. 2004

19. CIBSE. CIBSE/ Met Office hourly weather data. [available] www.cibse.org

20. McMullen, R. Environmental Science in Building. 5th ed 2002. Palgrave Macmillan, London p8

21. CIBSE. Climate Change and the Indoor Environment: Impacts and Adaptation. CIBSE TM36, 2005. Chartered Institute of Building Services Engineers, London. P14

22. CIBSE Guide A. Environmental Design. 1999

23 McLeod, R. Passivhaus Local House. MSc thesis, University of East London, 2007

24 Associates Staff Keller J. J., 2005, NIOSH "Pocket Guide to Chemical Hazards", Appendix A of the National Institute for Occupational Safety and Health

Table 1 – Dry and saturated thermo-physical properties for 180mm slump PRC mixes

	ρ_d	ρ_{sat}	n_{ap}	λ_{dry}	λ_{sat}	c_{dry}	c_{sat}
	kg/m^3	kg/m^3	%	W/(m K)	W/(m K)	J/(kg K)	J/(kg K)
Ref.	2288	2372	3.5	1.172	1.315	907	970
FR 10%	2113	2227	5.1	1.089	1.268	927	1019
FR20%	2056	2179	5.6	1.001	1.172	948	1049
FR30%	1913	2044	6.4	0.844	1.050	968	1083
CR10%	2063	2188	5.7	1.068	1.249	938	1040
CR20%	1905	2038	6.5	0.953	1.084	968	1084
CR30%	1772	1916	7.5	0.730	1.033	999	1134
CFR10%	2154	2280	5.5	1.071	1.274	933	1032
CFR20%	1991	2123	6.2	0.896	1.183	958	1069
CFR30%	1828	1979	7.6	0.678	1.062	983	1120

Table 2 – Dry and saturated thermo-physical properties for 120mm slump PRC mixes

	ρ_d	ρ_{sat}	n_{ap}	λ_{dry}	λ_{sat}	c_{dry}	c_{sat}
	kg/m^3	kg/m^3	%	W/(m K)	W/(m K)	J/(kg K)	J/(kg K)
Ref.	2296	2385	3.7	1.269	1.376	903	970
FR 10%	2162	2284	5.3	1.069	1.140	924	1020
FR20%	2039	2179	6.4	0.800	1.060	944	1060
FR30%	1878	2044	8.1	0.686	0.927	965	1112
CR10%	2091	2223	5.9	0.875	1.156	934	1041
CR20%	1944	2071	6.1	0.815	1.047	965	1075
CR30%	1754	1913	8.3	0.708	0.823	996	1146
CFR10%	2177	2238	5.4	1.100	1.083	929	1027
CFR20%	2016	2136	5.6	0.959	1.007	955	1056
CFR30%	1911	2031	5.9	0.848	0.996	980	1087

Table 3 – Dry and saturated thermo-physical properties for 65mm slump PRC mixes

	ρ_d kg/m^3	ρ_{sat} kg/m^3	n_{ap} %	λ_{dry} W/(m K)	λ_{sat} W/(m K)	c_{dry} J/(kg K)	c_{sat} J/(kg K)
Ref.	2311	2390	3.3	1.358	1.448	901	961
FR 10%	2179	2292	4.9	1.074	1.349	921	1010
FR20%	2081	2217	6.1	0.922	1.186	942	1053
FR30%	1934	2100	7.9	0.814	0.986	963	1107
CR10%	2126	2248	5.4	1.092	1.230	932	1030
CR20%	1956	2113	7.4	1.010	1.054	963	1098
CR30%	1806	1955	7.6	0.790	1.027	994	1132
CFR10%	2157	2273	5.1	0.942	1.251	927	1020
CFR20%	2022	2147	5.8	0.832	1.11	952	1057
CFR30%	1827	1982	7.8	0.779	1.008	978	1120

Table 4 – Dynamic thermal admittance properties for a 100mm thick external wall made using 180mm slump PRC mixes

	Y	ω	f	ϕ	F	ψ	U	κ	κ_{30}
	W/(m^2 K)	hr	-	hr	-	hr	W/(m^2 K)	kJ/(m^2 K)	kJ/(m^2 K)
Ref.	4.84	0.99	0.84	2.81	0.42	1.49	3.92	104	62
FR10%	4.71	1.01	0.85	2.75	0.44	1.43	3.82	98	59
FR20%	4.64	1.06	0.84	2.82	0.45	1.42	3.71	97	58
FR30%	4.43	1.14	0.84	2.88	0.48	1.38	3.46	93	56
CR10%	4.68	1.02	0.85	2.74	0.44	1.42	3.79	97	58
CR20%	4.53	1.07	0.85	2.74	0.46	1.37	3.64	92	55
CR30%	4.26	1.22	0.84	2.94	0.51	1.33	3.25	89	53
FCR10%	4.73	1.03	0.84	2.83	0.44	1.46	3.80	100	60
FCR20%	4.52	1.11	0.84	2.89	0.47	1.41	3.55	95	57
FCR30%	4.22	1.27	0.83	3.07	0.52	1.35	3.15	90	54

Table 5 – Dynamic thermal admittance properties for a 100mm thick external wall made using 120mm slump PRC mixes

	Y	ω	f	ϕ	F	ψ	U	K	κ_{30}
	W/(m^2 K)	hr	-	hr	-	hr	W/(m^2 K)	kJ/(m^2 K)	kJ/(m^2 K)
Ref.	4.90	0.95	0.85	2.74	0.41	1.49	4.02	104	62
FR10%	4.72	1.03	0.84	2.81	0.44	1.45	3.79	100	69
FR20%	4.44	1.18	0.83	3.04	0.48	1.42	3.39	96	58
FR30%	4.24	1.26	0.83	3.08	0.51	1.36	3.17	91	54
CR10%	4.53	1.13	0.83	2.97	0.47	1.43	3.50	98	59
CR20%	4.42	1.16	0.84	2.95	0.48	1.39	3.41	94	56
CR30%	4.22	1.23	0.84	2.95	0.51	1.33	3.21	87	52
FCR10%	4.76	1.01	0.84	2.81	0.44	1.46	3.83	101	61
FCR20%	4.59	1.08	0.84	2.83	0.46	1.41	3.65	96	58
FCR30%	4.45	1.14	0.84	2.91	0.48	1.39	3.47	94	56

Table 6 – Dynamic thermal admittance properties for a 100mm thick external wall made using 65mm slump PRC mixes

	Y	ω	f	ϕ	F	ψ	U	κ	κ_{30}
	W/(m^2 K)	hr	-	hr	-	hr	W/(m^2 K)	kJ/(m^2 K)	kJ/(m^2 K)
Ref.	4.96	0.92	0.85	2.70	0.40	1.45	4.10	105	63
FR10%	4.74	1.03	0.84	2.84	0.44	1.46	3.80	101	61
FR20%	4.59	1.10	0.83	2.94	0.46	1.44	3.59	99	59
FR30%	4.42	1.16	0.84	2.95	0.48	1.39	3.41	94	56
CR10%	4.73	1.02	0.84	2.79	0.44	1.45	3.82	100	60
CR20%	4.71	1.04	0.85	2.74	0.45	1.40	3.72	95	57
CR30%	4.35	1.17	0.84	2.89	0.49	1.35	3.37	90	54
FCR10%	4.63	1.10	0.83	2.97	0.46	1.46	3.62	101	60
FCR20%	4.48	1.16	0.83	3.01	0.48	1.42	3.45	97	58
FCR30%	4.33	1.18	0.84	2.90	0.49	1.35	3.35	90	54

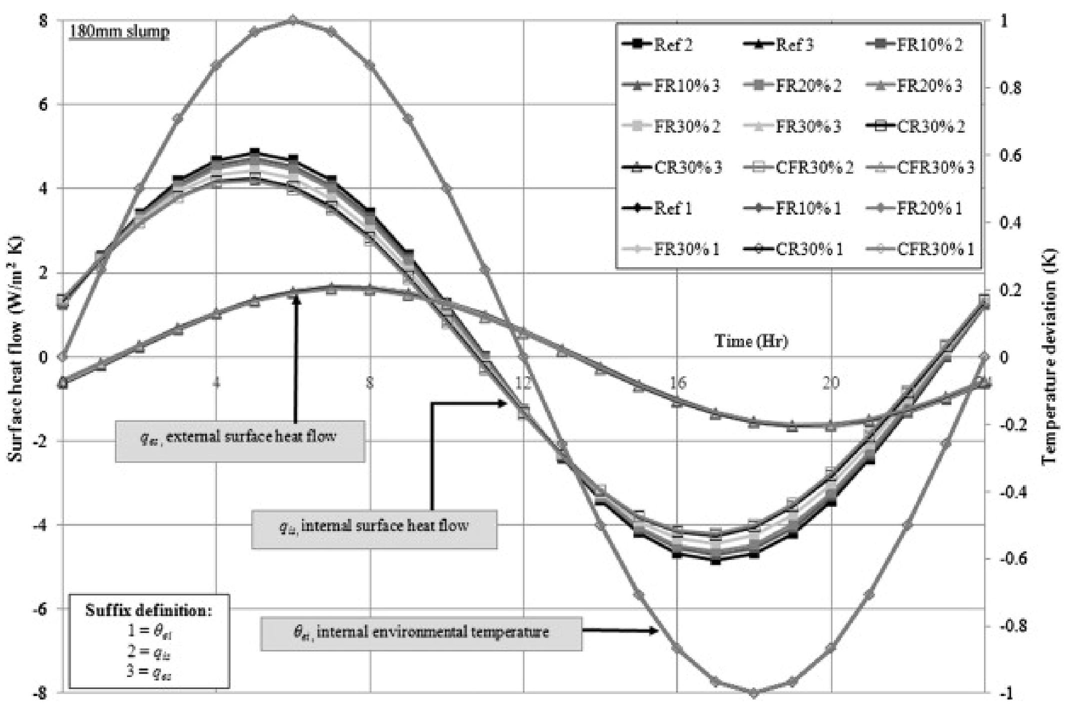

Fig. 1. Surface heat flow and internal environmental temperature fluctuation for 180 mm slump mix designs.

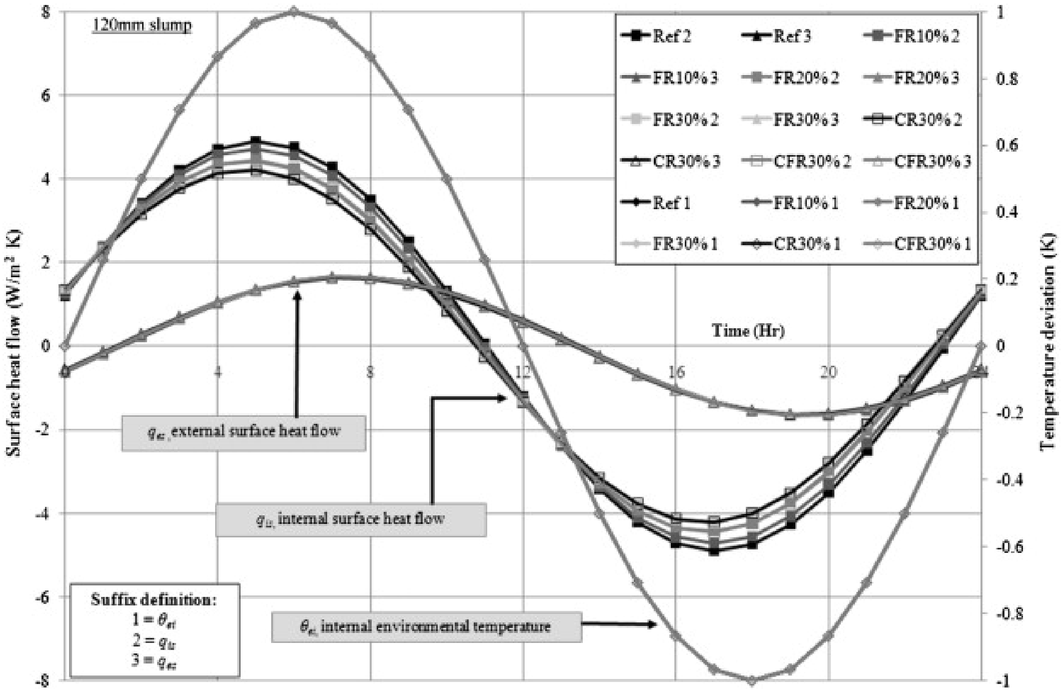

Fig. 2. Surface heat flow and internal environmental temperature fluctuation for 120 mm slump mix designs.

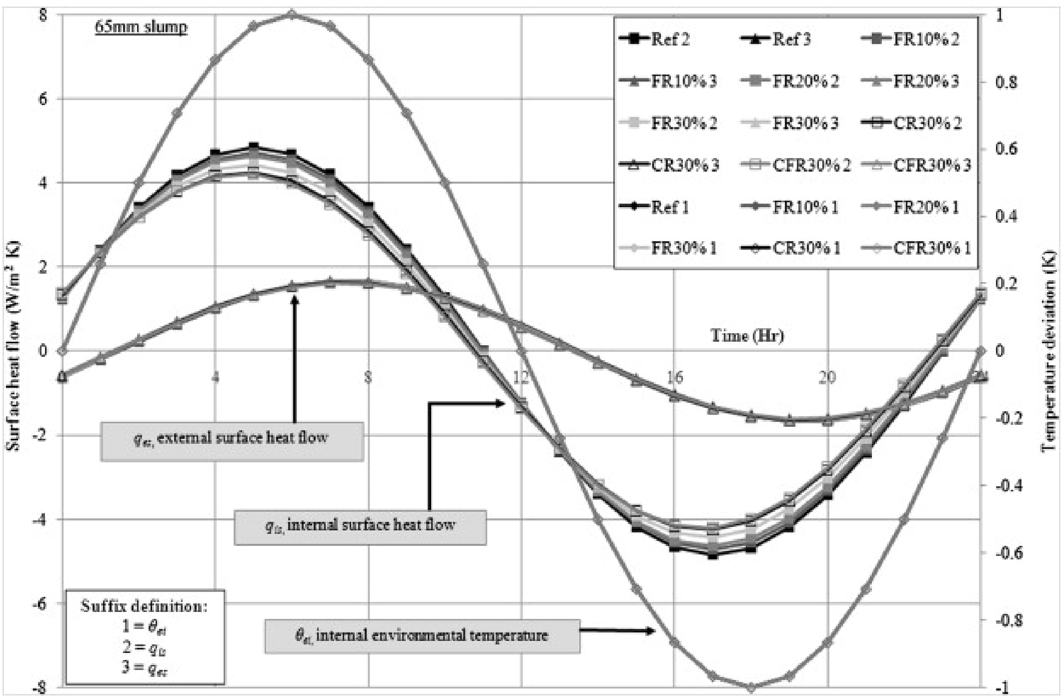

Fig. 3. Surface heat flow and internal environmental temperature fluctuation for 65 mm slump mix designs.

Material	External wall U-value
Ref 180	0.1453
30%FR 180	0.1439
30%CR 180	0.1431
30%CFR 180	0.1427
Ref 120	0.1451
30%FR 120	0.1424
30%CR 120	0.1426
30%CFR 120	0.1435
Ref 65	0.1454
30%FR 65	0.1433
30%CR 65	0.1431
30%CFR 65	0.1431

Floor	0.1000
Roof	0.1000
Glazing	0.6000
External doors	0.8000

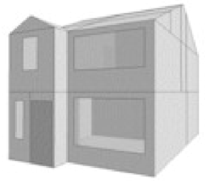

Thermal mass	Heavy
Construction:	
Ext. walls	Concrete block + mineral wool insulation + render
Solid floor	Concrete slab
Int. partitions	Concrete block + render

Fig. 4. Case study building typology and fabric thermal transmittance values.

	Layer Description	d m	λ W/(m·K)	ρ_d kg/m³	c_p J/(kg·K)
a	Dense render	0.012	0.41	1200	840
b	Concrete*	0.1	*	*	*
c	Glass woll ins.	0.26	0.04	200	670
d	Concrete*	0.1	*	*	*
e	Dense render	0.012	0.41	1200	840
f	Finishing plaster	0.002	0.5	1300	1000

R_{si}	0.117	(m²·K)/W
R_{so}	0.06	(m²·K)/W
R_T	6.923	(m²·K)/W
U (CIBSE)	0.1444	W/(m²·K)
U (EN ISO)	0.1446	W/m²·K
α_o	0.7	
α_i	0.55	
ε_o	0.9	
ε_i	0.9	

* mix design and thermophysical properties vary

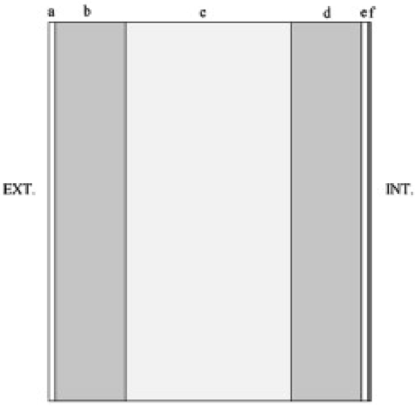

Fig. 5. Cross-sectional wall fabric design and assumed thermo-physical properties.

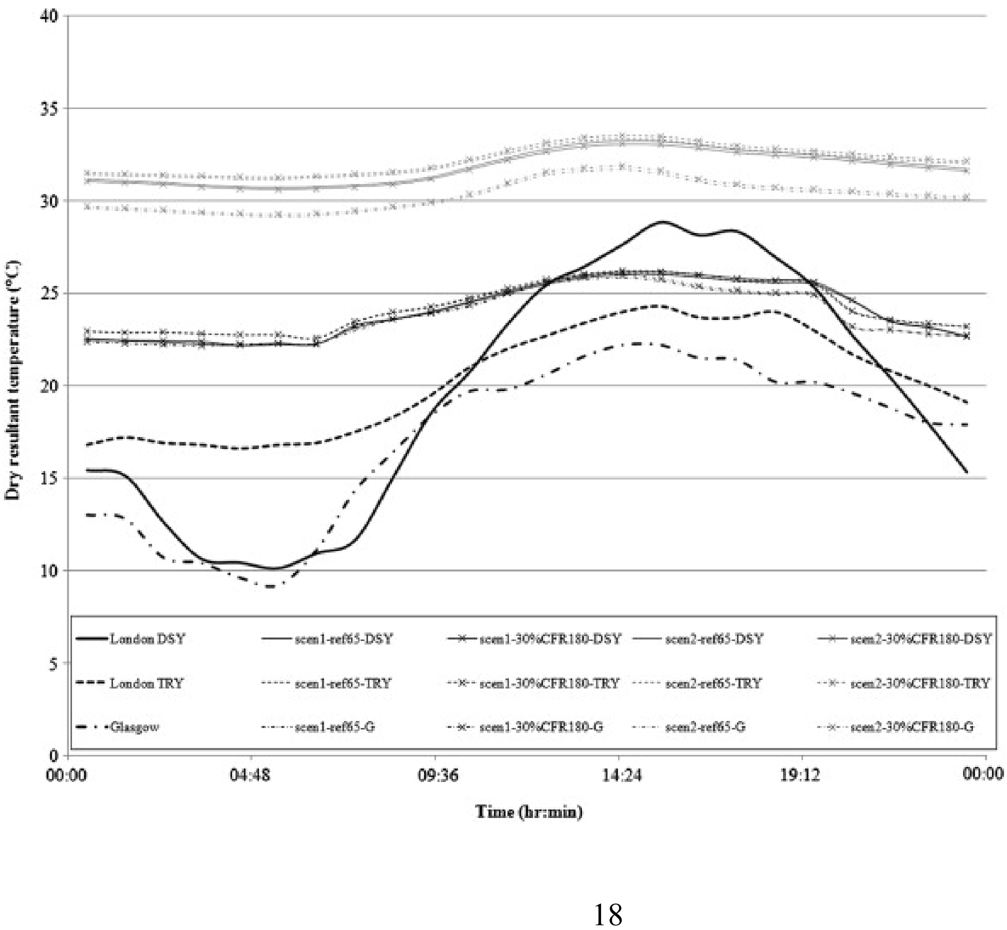

Fig. 6. Comparison between dry resultant temperature fluctuation and mix designs under London DSY/TRY and Glasgow climatic scenarios.

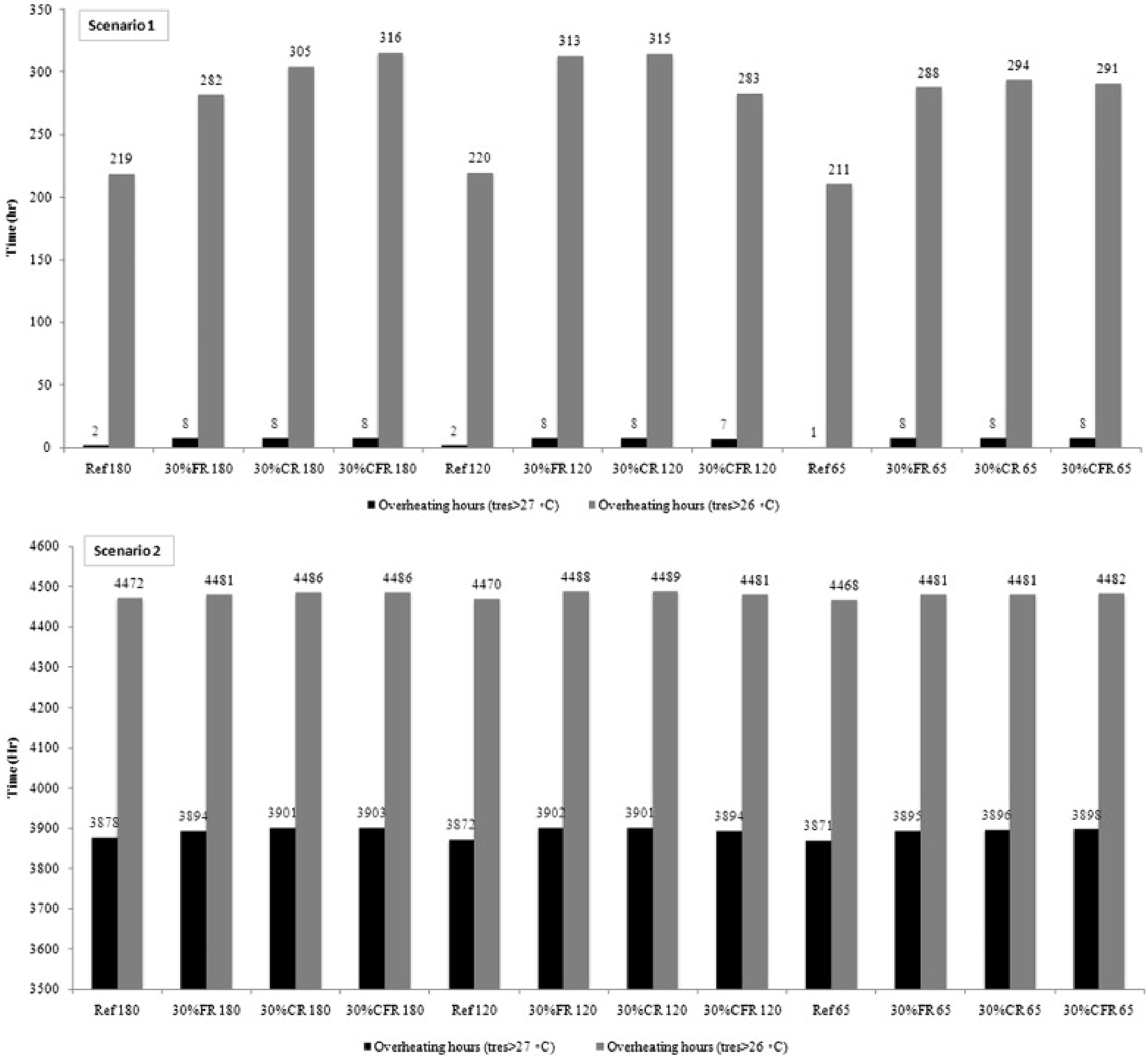

Fig. 7. Comparison between overheating hours and simulation scenarios 1 and 2.